

Melting-pressure and density equations of ^3He at temperatures from 0.001 to 30 K

Yonghua Huang and Guobang Chen

Cryogenics Laboratory, Zhejiang University, Hangzhou, 310027 China

(Received 21 June 2005; revised manuscript received 19 August 2005; published 18 November 2005)

Nonsegmented equations for melting pressure and density at temperatures from 0.001 K to 30 K have been developed to fit the reference data. The maximum and average deviations between the melting pressure equation and the totaling 298 reference data are 2.17% and 0.218%, respectively. For the density equations, the average deviations are 0.236% for the liquid side and 0.218% for the solid side. Both the melting pressure curve and melting density curves predicted by the submitted equations approach their minimums at about 0.315 K.

DOI: [10.1103/PhysRevB.72.184513](https://doi.org/10.1103/PhysRevB.72.184513)

PACS number(s): 67.90.+z, 64.30.+t, 67.80.-s, 67.55.-s

I. INTRODUCTION

A melting curve defines the limitation of a working substance existing in fluid state, which must be overstepped for solidification. So far, almost all the cryogenic fluids have their own standard or authoritative melting pressure equations in a wide range, except ^3He . In the past 50 years, many theoretical and experimental researches have been put on the melting curve of the last cryogenic fluid ^3He . Strong quantum effects at very low temperatures, no triple point existence, and superfluidity down to 2.6 mK, etc., have made ^3He significantly different from any other general cryogenic fluid. Such a number of interesting and unusual features of the melting curve of ^3He have stimulated many theoretical and experimental investigations. The melting pressure of ^3He is no longer monotone decreasing with temperature down to a very low degree. This implies that the melting curve would have a pressure minimum. In other words, the solid does not exist at pressures less than the minimum only even by cooling down to absolute 0 K.

In order to probe the anomalous melting properties of ^3He , we have collected quite a number of articles on the research activities of ^3He since 1949. This collection indicates that many measurements for the pressure and density (or molar volume) along the melting curve are available and united to cover a wide range. However, most of these measurements are in outdated unit systems and temperature scales as well. And the existing equations based on the measurements with narrow ranges of temperature, mostly from about 0.1 K to 1 K, cannot switch to each other smoothly. No independent and unitary equations have been reported to describe the properties on the melting curve of ^3He in a wide range. The traditional Simon melting equation, which has been successfully applied to other cryogenic fluids, no longer holds for ^3He because of the characteristics of this equation itself. In this work, the significant pressure-density-temperature characteristics of ^3He along the melting curve from 0.001 K to 30 K have been suggested and examined in detail, and nonsegmented equations for the melting pressure and density in question have been developed to fit the collected reference data.

II. REFERENCE DATA AND FORMULAS

Tables I–IV make brief summaries of the up-to-date research activities on pressure and density measurements, cal-

culations, and formulas along the melting curve of ^3He . Most of these data are experimental measurements and smoothed values directly given by the articles cited in the tables. The rest is obtained by picking up from the curves drawn in articles by using our self-programmed software. Tables II and IV list the searched equations in their original form, without any unit conversion. The coefficients of Rusby *et al.*'s equation in Table II can be found in the Appendix.

Before the least-squares fitting, procedures for converting temperatures measured on various scales to the currently accepted ITS-90 temperature scale and converting data from various sources to consistent units (SI units) for analysis have been completed first. The temperature scales are also listed in Tables I and III. Second, the data selection process is important and necessary. Systematic errors in the experimental data sets and methods of thermometry will certainly affect the quality of the state equation. To minimize the effects of such factors, care is taken to analyze each data set used in the development of the equation for consistency with independent measurements along the melting curve. Much effort has been performed to avoid using experimental data that contain large systematic errors in the fitting process. It should be pointed out that not all the listed data sets, but only those marked with “*” in Tables I and III have been used during the final fitting. Those not-used data given here are good references for the comparison in the following text of this paper. For melting pressures, it is found that observations at temperatures below 1 K are numerous and overlapped. Since the numerical differences between these early measurements due to temperature scales and methods of thermometry and manometry are worthwhile, it is complicated to convert all these data for the sake of consistency. Furthermore, it is not necessary to make such a conversion because Rusby *et al.*'s¹¹ small interval data published in 2003 are the most advanced data, which cover the whole range from 1 mK to 1 K and have been well accepted internationally. So, in our fitting program, only Rusby *et al.*'s data were adopted for the region below 1 K. At temperatures from 1 K to 30 K, reference data included in the least-squares fit were from Grilly and Mills^{2,4,9} and Sherman and Edeskuty,⁵ totaling 298 points. For melting densities, the guidelines for data selection are: (1) using numerical data listed in tables given in articles instead of data picked up from curves, and (2) data

TABLE I. Melting pressure measurements and smoothed values.

Year	Author	Ref.	Points	T range (K)	P range (MPa)	Temperature scale/Thermometer
1953	Weinstock <i>et al.</i>	1	29	0.1551–1.594	2.943–6.066	$T_{\text{CMN mag}}^{\text{a}}$
1955	Mills <i>et al.</i> *	2	Curve	1.44–29.85	5.69–343.94	1.9–5.2 K: v.p. ^4He T_{48} 5.2–12 K: Cu—Ci Fe thermoc. 12–24.5 K v.p. n— H_2 24.5–31 K: v.p. Ne
1959	Baum <i>et al.</i>	3	11	0.12–0.7	2.969–3.354	$T_{\text{CMN mag}}^{\text{b}}$
1959	Grilly and Mills*	4	29	1.332–30.184	5.061–348.607	<5.2 K: v.p. ^4He T_{58} 5.2–12 K: Cu—Ci Fe thermoc. 12–24.5 K: v.p. n— H_2 24.5–31 K: v.p. Ne
1960	Sherman and Edeskuty*	5	14	1.07–3.1		$T_{55\text{E}}$
1961	Mills <i>et al.</i>	6	10+Curve	0.3–1.2	2.929–4.5698	$T_{55\text{E}}$
1963	Anderson <i>et al.</i>	7	43+Curve	0.02–0.7	2.926–3.308	$T_{\text{CMN mag}}$
1969	Scribner <i>et al.</i>	8	31+Curve	0–0.7		>0.5 K: v.p. ^4He T_{58} and ^3He T_{62} <0.5 K: $T_{\text{CMN mag}}$ (T_{58} , T_{62} calibrated)
1971	Grilly*	9	18+Curve	0–1.8	2.937–6.858	T_{62} , v.p. ^3He
1986	Greywall	10	68	0.0009–0.25		$T_{\text{CMN mag}}$, NBS-CTS1983
2003	Rusby <i>et al.</i> *	11	220	0.001–1		PLTS-2000

^aCorrected to thermodynamic temperatures (Ref. 12).

^bCalibrated against ^4He vapor pressure temperature scale.

should cover the interested region as comprehensively as possible. Finally, only data from Grilly and Mills,^{4,6,9} and Sherman and Edeskuty⁵ are adopted. After converting the temperature scale and unit, a plot of these density data shows that they join with each other smoothly.

All the data marked with an asterisk in Tables I and III unite to cover a wide range from about 0.001 K to 30 K, which comes into being the basis of the derivation of our equations to be introduced in the following sections.

III. DERIVATION OF EQUATIONS

On the basis of the reference data in previous section, the authors have developed equations for pressure and densities on both liquid and solid sides along the melting curve.

A. Melting pressure equation

The anomalous melting properties of He^3 are heavily dependent upon the behavior of Fermi liquid and the spin sys-

TABLE II. Melting pressure formulas in literatures.

Year	Author	Ref	Equation	Units	T range (K)
1955	Mills <i>et al.</i>	2	$P=25.16+20.08201T^{1.517083}$	kg/cm ² ; K	1.844–29.88
1959	Grilly <i>et al.</i>	4	$P=27.256-0.64696T+16.0205T^2-1.39505T^3$	kg/cm ² ; K	1.2-3.1 α Solid→Liquid
			$P=3.873+30.5539T+4.08176T^2$	kg/cm ² ; K	3.2–4.4 β Solid→Liquid
1960	Sydoriak <i>et al.</i>	13	$P=28.91+32.20(T-0.330)^2$	atm; K	0.3–0.5
1960	Sherman <i>et al.</i>	5	$P=24.559+16.639T^2-2.0659T^3+0.11212T^4$	atm; K	1.07–3.1
1961	Mills <i>et al.</i>	6	$P=28.91+32.20(T-0.330)^2$	atm; K	0.33–1.2
1963	Anderson <i>et al.</i>	7	$P=425+485(0.3191-T)^2+546.5(0.3191-T)^3$	psi; K	0.03–0.4
1968	Zeisse <i>et al.</i>	14	$P=29.107+0.25537(t)^2-0.05700(t)^3+0.01625(t)^4$ $100t=T-299.028$	atm; mK	0.012–0.6
1969	Scribner <i>et al.</i>	8	$P=28.94+25.86(T-0.318)^2$	atm; K	0.26–0.38
1986	Greywall	10	$P_m - P_A = \sum_{n=-3}^{+5} a_n(T)^n$	bar; mK	0.0009–0.25
2003	Rusby <i>et al.</i>	11	$P_m = \sum_{i=-3}^{+9} a_i(T)^i$	MPa; K	0.001–1

TABLE III. Density measurements and calculations along the melting curve of ^3He .

Year	Author	Ref.	Liquid Points	Solid Points	T range (K)	Temperature scale
1959	Grilly and Mills*	4	29	29	1.332–30.184	<5.2 K: v.p. ^4He T_{58} 5.2–12 K: Cu—Ci Fe thermoc. 12–24.5 K: v.p. n- H_2 24.5–31 K: v.p. Ne
1960	Sherman and Edeskuty*	5	24	0	0.05–3.99	T_{55E}
1960	Sydoriak <i>et al.</i>	13	Curve	Curve	0.32–1.2	<5.2 K: v.p. ^4He T_{58}
1961	Mills <i>et al.</i> *	6	10+Curve	10+Curve	0.33–1.2	T_{55E}
1963	Anderson <i>et al.</i>	7	16	16	0.02–0.32	$T_{CMN\ mag}$
1971	Grilly*	9	34	34	0.02–1.8	T_{62} , v.p. ^3He

tems of the solid and liquid phases. Liquid ^3He obeys Fermi-Dirac statistics. The departure from classical behavior occurs roughly at the temperature where the thermal de Broglie wavelength is on the order of the mean interparticle spacing. This temperature is on the order of 1 K for liquid ^3He (depending on the density). Well below this temperature (called the Fermi degeneracy temperature T_F), the specific heat and the entropy will both be linear functions of the absolute temperature. On the other hand, in the range of temperatures above 0.01 K, the nuclear spins of the ^3He atoms comprising the solid should be almost fully disordered. For spin 1/2 nuclei this required that the solid entropy S_s should be equal to $R \ln 2$ per mole. Based on these considerations, as shown in Fig. 1, one is able to explore the implications of the liquid-solid phase equilibrium by the famous Clausius-Clapeyron equation,

$$\frac{dp_m}{dT} = \frac{\Delta S_m}{\Delta V_m} = \frac{S_l - S_s}{V_l - V_s}. \quad (1)$$

For ^3He , the molar volume of liquid V_l is always greater than that of solid V_s , so the denominator is always positive. On the other hand, the numerator will change sign as one cools into the Fermi degenerate region because S_l will become less than the constant solid entropy $S_s = R \ln 2$ corresponding to random spin orientation, so at the lowest temperatures the slope of the melting curve becomes negative. At the higher temperatures, the entropy of the liquid will be greater than

$R \ln 2$ per mole so that the slope of the melting becomes positive. Figure 1 implies that the melting curve will have a minimum at the place where the liquid entropy curve intersects the solid entropy curve.

The authors find it difficult to derive an exact theoretical equation that excellently represents the above-mentioned slope behavior of the melting pressure curve for ^3He . Instead, various general polynomial equations and their combinations with exponential terms were tried empirically. Unfortunately, none of the equation forms that had been successfully applied to other cryogenic fluids can perfectly fit the selected reference data of ^3He . On the other hand, it is not difficult to find that the pressure of ^3He varies from about 3 MPa to 400 MPa when the temperature increases from 0.001 K to 30 K. Such a large variation of the numerical magnitudes may require using logarithm functions. At the same time, we noticed that a rational equation in the form of a polynomial divided by a polynomial has two branches on both sides of its vertical asymptote. The tendency of the left branch meets the requirement in question. However, the melting-pressure equation should also be reasonably simple so as to be useful in thermodynamic calculations. Obviously, more terms may be put into an equation to get better agreement with the collected data, but complexity is the penalty. After many trials, the following empirical equation is suggested for the melting-pressure behavior of ^3He as a function of temperature,

$$\ln(P) = \frac{c_1 + c_3 \ln T + c_5 (\ln T)^2 + c_7 (\ln T)^3 + c_9 (\ln T)^4 + c_{11} (\ln T)^5}{1 + c_2 \ln T + c_4 (\ln T)^2 + c_6 (\ln T)^3 + c_8 (\ln T)^4 + c_{10} (\ln T)^5}, \quad (2)$$

TABLE IV. Correlations for density along the melting curve of ^3He .

Year	Author	Ref	Equation	Units	P range
1959	Grilly <i>et al.</i>	4	$V_f = -3.2482 + 51.1102(P_m + 1.075)^{-0.161532}$	kg/cm ² ; cm ³ /mol	50–3555 kg/cm ²
			$\Delta V_m = 1.56464 - 0.39023 \log_{10}(P_m - 29.998)$	kg/cm ² ; cm ³ /mol	51–128 kg/cm ²
			$\Delta V_m = 1.51053 - 0.30825 \log_{10}(P_m - 42.581)$	kg/cm ² ; cm ³ /mol	146–3555 kg/cm ²

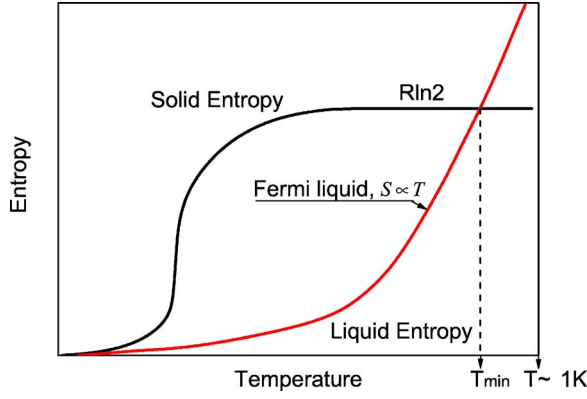


FIG. 1. (Color online) An idealized sketch map of the entropy of liquid and solid ^3He along the melting curve.

where P is melting pressure in MPa, and T is temperature in K. The coefficients c_1 – c_{11} are listed in Table V. The suggested working range for this melting pressure equation is 0.001 K–30 K, however, an extension of Eq. (2) to higher temperatures up to 35 K is also dependable. The melting pressure will be a very high value of 550 MPa at 40 K, which is hard to realize in actual experiments. For Eq. (2), when temperature $T \rightarrow +0$, that is $\ln(T) \rightarrow -\infty$, $\ln(P)$ approaches its limit $c_{11}/c_{10} = 1.3486$, that is $P = 3.852$ MPa. It should be noted that the solid ^3He has two different phases, α (bcc structure) and β (hcc structure), as show in Fig. 2. The measurements by Grilly and Mills⁴ on the solid α -liquid boundary and solid β -liquid boundary join smoothly. The solid α -solid β transition line intersects with the melting curve at a point with the temperature 3.154 K (ITS-90 scale). It can be seen that the solid line plotted in Fig. 2 predicted by Eq. (2) smoothly and continuously connects the measurements on the coexistence line of liquid and both α and β solid.

B. Density equations along the melting curve

It is interesting to see that the shape of density plots along the melting curve looks quite similar to that of the melting

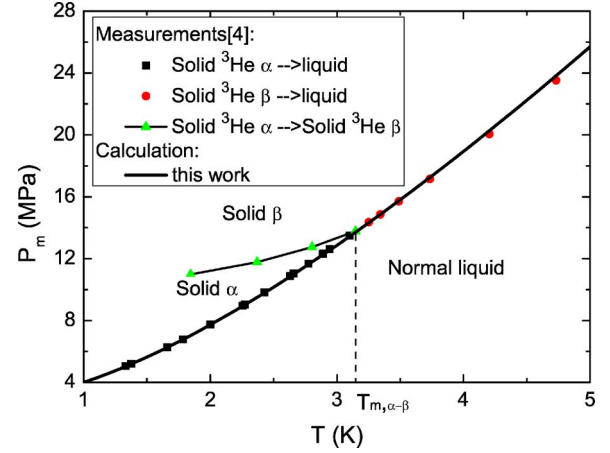


FIG. 2. (Color online) Transition between two crystalline phases of solid ^3He and normal liquid ^3He .

pressure. In view of the successful application of the rational form to melting pressure, the density equations for both the liquid and solid along the melting curve of ^3He are also in a similar form of rational expression except without any logarithm functions due to the small numerical magnitude of the density variation,

$$\rho = \frac{c_1 + c_3 T + c_5 T^2 + c_7 T^3 + c_9 T^4 + c_{11} T^5}{1 + c_2 T + c_4 T^2 + c_6 T^3 + c_8 T^4 + c_{10} T^5}, \quad (3)$$

where ρ is the liquid or solid density along the melting curve, unit in kg/m^3 ; and T is temperature in K. Different coefficients, also listed in Table V, are obtained for liquid and solid respectively.

IV. RESULTS AND DISCUSSION

A. Accuracy of the melting pressure equation

Figure 3 shows the agreement of the calculations by Eq. (2) (solid line) with the experimental and calculated data listed in Table I. The area around the P_{\min} has been enlarged

TABLE V. Coefficients for Equations (2) and (3).

Coefficients	Equation (2)	Equation (3)	
		Liquid side	Solid side
c_1	1.387061	119.026135	125.106337
c_2	-0.47739621	0.26598247	0.744874167
c_3	$1.173634148 \times 10^{-2}$	8.959606	63.4602862
c_4	0.329447888	0.259048	$5.69419341 \times 10^{-2}$
c_5	0.563607496	73.0945524	60.44224356
c_6	-0.09599502	-0.35192157	$9.606419123 \times 10^{-2}$
c_7	-0.111889	-59.347	-15.834
c_8	$1.36493847 \times 10^{-2}$	0.15613338	0.17301133
c_9	$1.570888538 \times 10^{-2}$	19.37724	30.6121475
c_{10}	$-7.7718566 \times 10^{-4}$	3.8934088×10^{-3}	$3.11169498 \times 10^{-3}$
c_{11}	$-1.045706897 \times 10^{-3}$	1.9364125	1.699408157

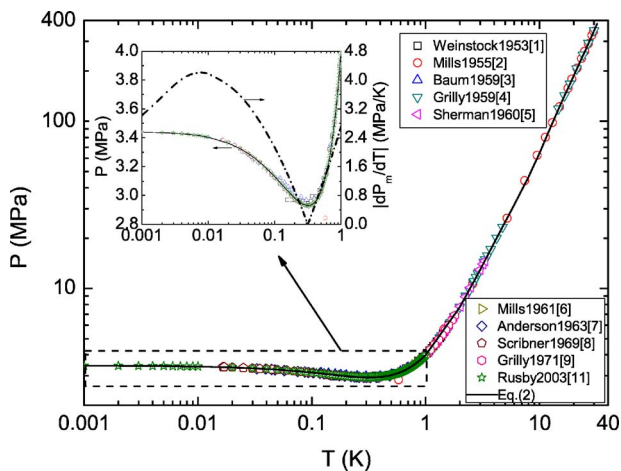


FIG. 3. (Color online) Melting pressure of ^3He vs temperature: solid curve shows calculated results by Eq. (2).

to show the specialty of the ^3He melting pressure. Figure 4 gives the relative residuals between the calculations by the equation and the measurements.

It can be seen from Figs. 3 and 4 that Eq. (2) well represents the characteristics of the melting pressure of ^3He . The maximum and average residuals in percent between Eq. (2) and the 298 reference data in the temperature range from 0.001 K to 30 K are 2.17% and 0.218%, respectively. In the range 0.001 K–1 K, our melting pressure equation agrees with the equation presented by Rusby *et al.*¹¹ within 0.16%, as shown in Fig. 5. Rusby *et al.*'s equation has been used to define the Provisional Low Temperature Scale from 0.9 mK to 1 K, which was adopted by the Comité International des Poids et Mesures in October 2000.

Another important characteristic of Eq. (2) to be examined is the phenomenon of the melting-pressure minimum. When ^3He was first solidified in 1951 by Osborne *et al.*,^{15,16} the observation of a melting pressure minimum¹⁷ was precluded due to the measurement technique, which resulted in the capillary leading to the sample chamber blocked with solid. Consequently, observation of $P > P_{\min}$ at $T < T_{\min}$ by

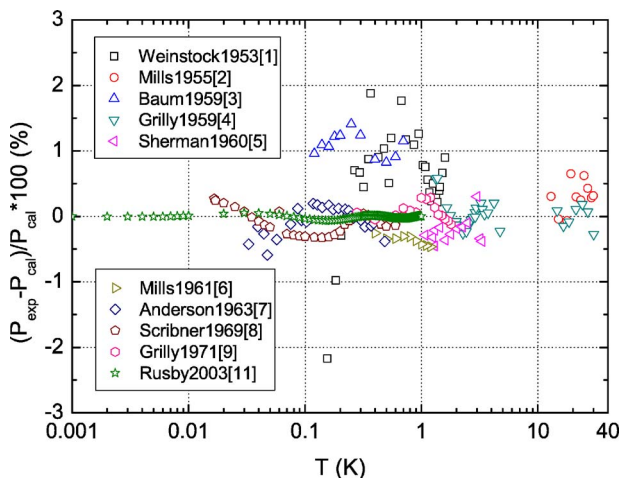


FIG. 4. (Color online) Residuals between the calculated results by Eq. (2) and reference data.

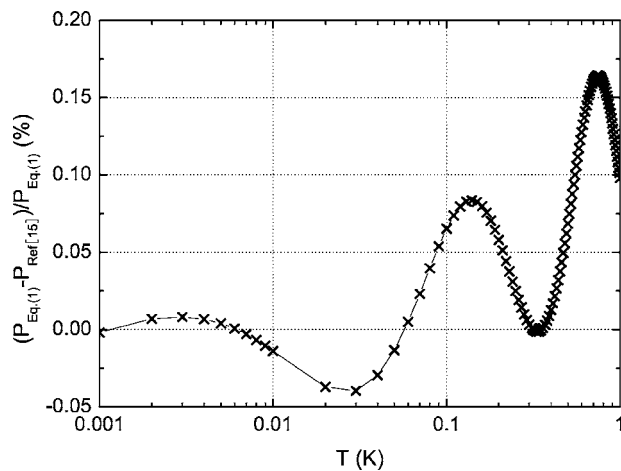


FIG. 5. The residuals between Eq. (2) and Rusby *et al.*'s equation.

sensing the pressure in the capillary becomes impossible. Baum *et al.*³ directly detected the minimum in $P_m(T)$ using a variation of the blocked-capillary procedure. At 1.2 K the sample chamber was filled to a pressure that would ensure the maintenance of two-phase equilibrium over the region to be investigated. At the same time, Bernardes and Primakoff^{18,19} led in 1959 to a fairly accurate prediction of an alignment temperature 0.37 K for the pressure minimum due to crystal lattice theory of ^3He . A number of other investigations^{7,20} employing the blocked capillary as well as different techniques have amply substantiated the minimum in $P_m(T)$. Table VI lists a brief summary of determinations of the location of the minimum of the melting curve of ^3He .

The melting pressure minimum P_{\min} and its corresponding temperature T_{\min} calculated by Eq. (2) with $dP/dT=0$ are 2.93113 MPa and 0.31586 K, respectively. These values are in good quantitative agreement with those latest researches listed in Table VI, especially the most recent results given by Rusby *et al.*¹¹ as the PLTS-2000 scale definition.

B. The performance of the density equations

Figures 6 and 7 show the agreement of Eq. (3) with the melting-density reference data versus temperature. The average deviations for the liquid and solid sides are 0.236% and 0.218% respectively. The behavior of liquid melting density ρ_L at $T < 1$ K is illustrated clearly in Fig. 6. One should notice that measurements in the liquid by Grilly⁹ are obviously greater than others below about 0.7 K. The fact of the other results bearing the same kind of deviation below 0.3 K is that Scribner and Adams *et al.* used the Mills' data for calibration. Equation (3) bias toward the Mills' data, whose error was estimated at less than 0.1%.

The density minimum calculated by Eq. (3) for liquid along the melting curve locates at 0.3152 K, which leads to $\rho_{L,\min} = 115.8533 \text{ kg/m}^3$; for solid, $T_{S,\min} = 0.3151 \text{ K}$, $\rho_{S,\min} = 121.2091 \text{ kg/m}^3$. It is interesting to find that these temperatures are almost the same as that of the melting-pressure curve predicted by Eq. (2).

C. The relationship between the melting pressure and density

Of even more concern, when combining Figs. 3, 6, and 7, is the trend similarity of melting-density curves and melting-

TABLE VI. Summary of determinations of the location of the minimum of the melting curve of ^3He .

Year	Author	Ref.	P_{\min} (MPa)	T_{\min} (K)	Method
1959	Baum <i>et al.</i>	3	2.96882 ± 0.01^a	0.32 ± 0.004	Resistance strain gauge pressure measurement; powdered cerium magnesium nitrate (CMN) sphere thermometry
1961	Mills <i>et al.</i>	6	2.92931 ± 0.002	0.323 ± 0.005	Spring-loaded bellows, differential-pressure measurement; corrected ^3He vapor pressure thermometry
1961	Lee <i>et al.</i>	21	2.94958 ± 0.01	0.32 ± 0.01	Observation of density
1961	Anderson <i>et al.</i>	20	2.93372 ± 0.01	...	Melting of plug
1963	Anderson <i>et al.</i>	7	2.93336 ± 0.007	0.319 ± 0.005	Resistance strain gauge pressure measurement; observations of compressional cooling; powdered CMN, cylinder thermometry
1968	Zeisse <i>et al.</i>	14	2.94856 ± 0.03	0.299 ± 0.021	Capacitance strain gauge; NMR thermometry
1969	Scribner <i>et al.</i>	8	2.93235 ± 0.003	0.318 ± 0.006	Capacitance strain gauge pressure measurements; powdered CMN, cylinder thermometry
1971	Grilly <i>et al.</i>	9	2.93153 ± 0.003	0.319 ± 0.003	
2003	Rusby <i>et al.</i>	11	2.93113	0.31524	Calculation by a correlation
2005	This paper		2.93113	0.31586	Calculation by Eq. (2)

^aReference 7 has pointed out that ~ 0.03 MPa systematic error appears in the pressure measurements of Baum *et al.*

pressure curve. This implies an interesting relationship between these two properties along the melting curve.

According to the Clausius-Clapeyron equation [Eq. (1)], the slope of the melting pressure is directly associated with the relative magnitudes of the molar volume (or density) change along the melting curve. As mentioned in Sec. III A, at not sufficiently high as well as not sufficiently low temperatures, we shall assume that the solid entropy is $R \ln 2$ over the entire region of interest. Under this assumption, we can take both the solid expansion coefficient and specific heat to be zero. Hence, the solid molar volume will be a function of pressure only. This reflects the curve similarity between the density and pressure.

The consistency of melting-pressure minimum and density minimum can be explained as following. In thermodynamics, the thermal expansion coefficient α can be expressed as

$$\alpha = \beta \frac{dP_m}{dT} - \frac{1}{\rho} \frac{d\rho}{dT} \quad (4)$$

or

$$\alpha = \left(\beta - \frac{1}{\rho} \frac{d\rho}{dP_m} \right) \frac{dP_m}{dT}, \quad (5)$$

where β is the compressibility coefficient. From the observation that β remains finite and $d\rho/dP_m$ is nearly constant as $P_m \rightarrow P_{\min}$, then according to Eq. (5), $\alpha \rightarrow 0$ as $T \rightarrow T_{\min}$. From Eq. (4), $d\rho/dT$ must also become zero at T_{\min} . These clues help to demonstrate the essential correlations or thermodynamic consistency between the pressure and density along the melting curve.

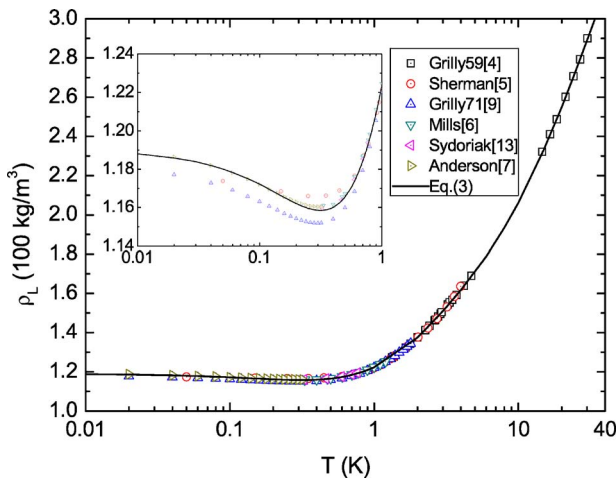


FIG. 6. (Color online) Eq. (3) fits the melting density reference data in the liquid side.

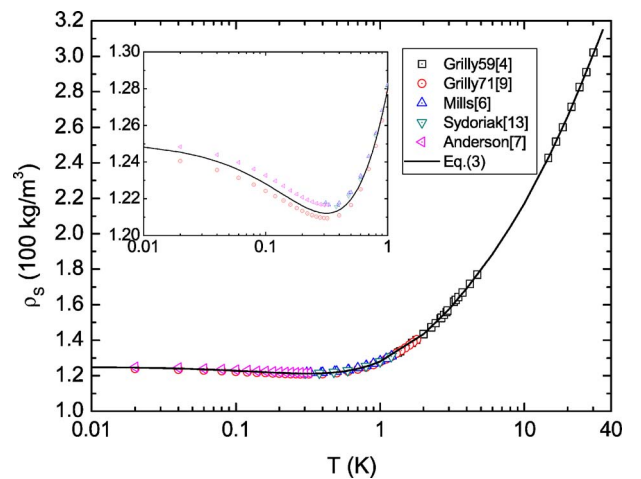


FIG. 7. (Color online) Eq. (3) fits the melting density reference data in the solid side.

V. SUMMARY

Nonsegmented equations for ^3He melting pressure and density in the temperature range from 0.001 K to 30 K have been developed to fit the measurements. The maximum and average deviation in percent between the melting pressure equation and the 298 reference data are 2.17% and 0.218%, respectively. For the density equations, the average deviation is 0.236% for the liquid side and 0.218% for the solid side. Both the melting-pressure equation and the melting-density equations predict almost the same tem-

perature, about 0.315 K at the pressure and/or density minimum.

ACKNOWLEDGMENT

This project is financially supported by the National Natural Science Foundation of China (No. 50376055).

APPENDIX

The Coefficients for Rusby *et al.*'s equation as referenced in Table II, are as follows:

$$\begin{aligned} a_{-3} &= -1.3855442 \times 10^{-12} \\ a_{-2} &= 4.5557026 \times 10^{-9} \\ a_{-1} &= -6.4430869 \times 10^{-6} \\ a_0 &= 3.4467343 \times 10^0 \\ a_1 &= -4.4176438 \times 10^0 \end{aligned}$$

$$\begin{aligned} a_2 &= 1.5417437 \times 10^1 \\ a_3 &= -3.5789853 \times 10^1 \\ a_4 &= 7.1499125 \times 10^1 \\ a_5 &= -1.0414379 \times 10^2 \\ a_6 &= 1.0518538 \times 10^2 \end{aligned}$$

$$\begin{aligned} a_7 &= -6.9443767 \times 10^1 \\ a_8 &= 2.6833087 \times 10^1 \\ a_9 &= -4.5875709 \times 10^0 \end{aligned}$$

¹B. Weinstock, B. M. Abraham, and D. W. Osborne, Phys. Rev. **89**, 787 (1953).

²R. L. Mills and E. R. Grilly, Phys. Rev. **99**, 480 (1955).

³J. L. Baum, D. F. Brewer, J. G. Daunt, and D. O. Edwards, Phys. Rev. Lett. **3**, 127 (1959).

⁴E. R. Grilly and R. L. Mills, Ann. Phys. (N.Y.) **8**, 1 (1959).

⁵R. H. Sherman and F. J. Edeskuty, Ann. Phys. (N.Y.) **9**, 522 (1960).

⁶R. L. Mills, E. R. Grilly, and S. G. Sydorik, Ann. Phys. (N.Y.) **12**, 41 (1961).

⁷A. C. Anderson, W. Reese, and J. C. Wheatley, Phys. Rev. **130**, 1644 (1963).

⁸R. A. Scribner, M. F. Panczyk, and E. D. Adams, J. Low Temp. Phys. **1**, 313 (1969).

⁹E. R. Grilly, J. Low Temp. Phys. **4**, 615 (1971).

¹⁰D. S. Greywall, Phys. Rev. B **33**, 7520 (1986).

¹¹R. L. Rusby, M. Durieux, A. L. Reesink, R. P. Hudson, G.

Schuster, M. Kühne, W. E. Fogle, R. J. Soulen, and E. D. Adams, AIP Conf. Proc. **684**, 77 (2003).

¹²A. H. Cooke, Proc. Phys. Soc., London, Sect. A **62**, 269 (1949).

¹³S. G. Sydorik, R. L. Mills, and E. R. Grilly, Phys. Rev. Lett. **4**, 495 (1960).

¹⁴C. R. Zeisse, Phys. Rev. **173**, 301 (1968).

¹⁵D. W. Osborne, B. M. Abraham, and B. Weinstock, Phys. Rev. **82**, 263 (1951).

¹⁶B. Weinstock, B. M. Abraham, and D. W. Osborne, Phys. Rev. **85**, 158 (1952).

¹⁷T. R. Roberts and S. G. Sydorik, Phys. Rev. **93**, 1418 (1954).

¹⁸N. Bernardes and H. Primakoff, Phys. Rev. Lett. **2**, 290 (1959).

¹⁹N. Bernardes and H. Primakoff, Phys. Rev. **119**, 968 (1960).

²⁰A. C. Anderson, G. L. Salinger, W. A. Steyert, and J. C. Wheatley, Phys. Rev. Lett. **7**, 295 (1961).

²¹D. M. Lee, H. A. Fairbank, and E. Walker, Phys. Rev. **121**, 1258 (1961).